ACS OMEGA

Open Access

http://pubs.acs.org/journal/acsodf

Article

Postsynthetic Modification of Amine-Functionalized MIL-101(Cr) Metal−Organic Frameworks with an EDTA−Zn(II) Complex as an Effective Heterogeneous Catalyst for Hantzsch Synthesis of Polyhydroquinolines

Ahmad Nikseresht,* Fatemeh Ghoochi, and Masoud Mohammadi*

Cite This: *ACS Omega* 2024, 9, 28114−28128

Read Online

ACCESS | Metrics & More | Article Recommendations | Supporting Information

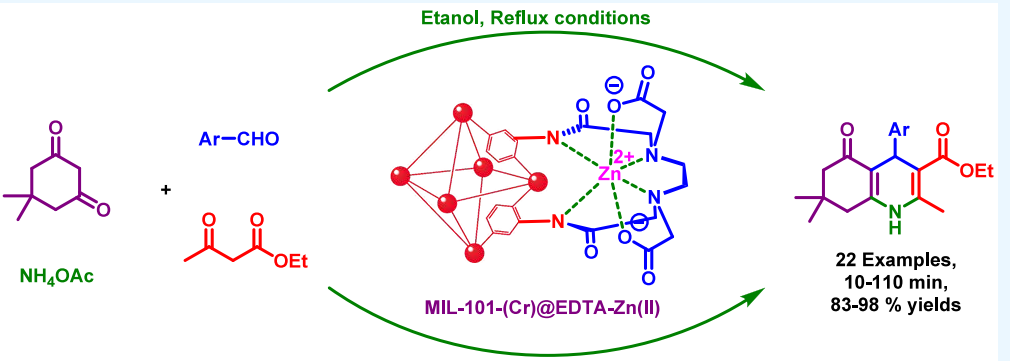

ABSTRACT: The present work aims at preparing the EDTA−Zn(II) complex—supported on the amine-functionalized MIL-101(Cr) MOF—as a new and effective heterogenized catalyst. The optimization of the hydrothermal process shows that 120 °C is the best condition to grow the MIL-101(Cr)−NH_2 MOF crystals. Moreover, regarding the use of the postsynthetic modification (PSM) method, hexadentate EDTA was grafted on this support via a simple aminolysis process before further coordinating it with Zn ions to create the corresponding Zn(II) catalytic complex. The catalytic activity of this compound was then investigated in the context of a one-pot synthesis of polyhydroquinolines. This approach has a number of advantages including the following: the use of a solvent that is not hazardous, applying a porous catalyst that is inexpensive, secure, and recyclable; rapid reaction times, high levels of efficiency, and the simplicity of MOF catalyst separation. Accordingly, the process in question can be given the label of "green chemistry".

1. INTRODUCTION

Considering heterogeneous catalysis, metal−organic frameworks (MOFs) have been developed into a popular concept.[1−3] They are self-assembled by the coordination of metal cations or clusters acting as nodes and organic ligands acting as linkers.[4,5] As a result of the tenability of pore size, chemical tenability, topologies, and a very substantial inner surface area, significant metallic dispersion is to be anticipated for MOFs, which will convert them into a unique class of functional materials with potential applications in catalysis.[6−10] Moreover, the thin micropore distribution of MOFs may result in monodisperse nanometric metallic clusters, which are of great importance for catalytic activity and selectivity.[11−15] The highly programmable organic and inorganic components of MOFs distinguish them from other porous inorganic materials like zeolites.[16−18] In this sense, organic moieties allow them to be customized with various functional groups (i.e., acid, bases and metal complexes), also known as a postsynthetic modification (PSM) process, to improve their characteristics for various applications, especially in the field of catalysis.[19−23] MIL-101(Cr)−NH_2 (MIL stands for Materials of Institute Lavoisier), which was constructed using chromium clusters and a 2-amino terephthalate ligand, is one of the best-known MOFs that have been previously produced.[24−26] The functionalization of this MOF can be achieved through the PSM method on its active amine groups, offering a significant technique to enhance its capacity for catalytic applications.[26,27]

Ethylenediaminetetraacetic acid (EDTA) is classified as a hexadentate ligand that has six coordinative sites, four of which

Received: February 4, 2024
Revised: May 30, 2024
Accepted: June 7, 2024
Published: June 21, 2024

Scheme 1. Stepwise Synthesis of MIL-101(Cr)@EDTA−Zn(II) Complex (schematic structures)

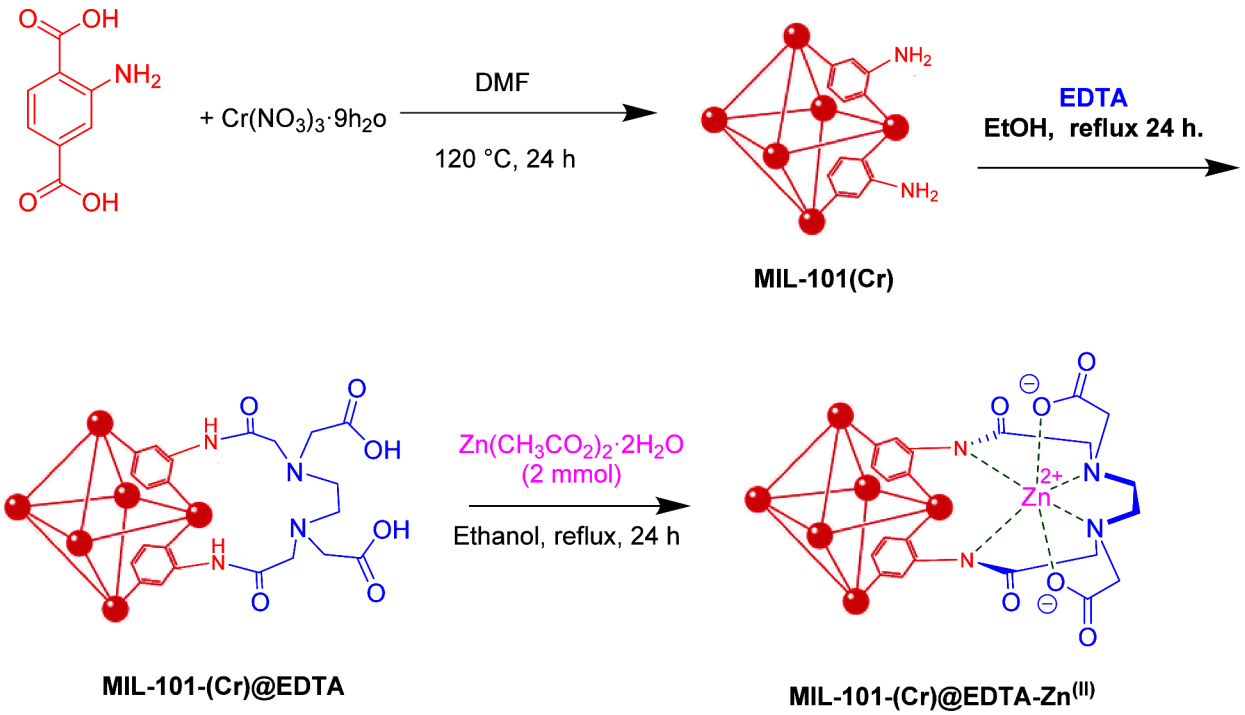

are occupied by oxygen atoms that come from carboxyl groups, and the rest are occupied by nitrogen atoms, in which the lone pairs of electrons have the ability to coordinate to the positively charged metal ions. Moreover, it can form complexes with almost any kind of metal ion.[28−30] It is worth mentioning that the presence of four carboxylic acid functionalities in this structure provide immobilization on solid supports. Notably, several research projects in this field aim to come up with materials that can be used for a wide range of purposes.[31−34] In this study, we introduce a novel approach for supporting EDTA onto the MIL-101(Cr)−NH_2 MOF, distinct from conventional methods commonly discussed in the literature. While previous works have predominantly focused on utilizing ethylenediaminetetraacetic dianhydride (EDTA−dianhydride)[35] or employing activators such as 1-ethyl-3-(3-(dimethylamino)propyl) carbodiimide hydrochloride (EDC·HCl) and *N*-hydroxysuccinimide (NHS) for EDTA immobilization,[36] our methodology offers a significant departure from these conventional techniques. In this research, we explore the feasibility of stabilizing EDTA on MIL-101(Cr)−NH_2 MOF through a straightforward aminolysis process. Here, the carboxylic acid groups of EDTA interact with the surface amine groups followed by complexation with Zn ions to form the corresponding MIL-101(Cr)@EDTA−Zn(II) complex for catalytic applications. This approach offers a robust and stable method without the necessity for additional chemical modifiers. This innovative approach not only streamlines the synthesis process but also avoids the side reactions and enhances the catalytic performance and reproducibility, opening avenues for broader applications in various chemical reactions. By elucidating these key differences, we underscore the unique advantages and potential of our EDTA-stabilized MIL-101(Cr)−NH_2 catalyst compared to existing materials, paving the way for its widespread adoption in catalysis and beyond.

Due to the wide variety of pharmacological and biological characteristics of polyhydroquinolines with a 1.4-dihydroquinoline core in their structure, these compounds are regarded as significant organic substances.[5,37−39] As discussed by Kazemi and Mohammadi, different catalysts have been described in the earlier literature for the synthesis of polyhydroquinoline and its derivatives due to its broad variety of uses in diverse fields.[40] Despite having certain benefits in the synthesis of polyhydroquinoline derivatives, each of these approaches typically suffered from a slow and inefficient process, a poor yield, catalyst toxicity, a constrained range of reactions, harsh reaction conditions, etc. In order to circumvent such restrictions, there is a need to develop novel catalysts.

Given the aforementioned concerns, herein, the PSM method was used to synthesize a new EDTA-based catalytic complex on MIL-101(Cr)−NH_2 MOF. Afterward, because metal complexes act as catalysts in multicomponent reactions, it was also used as an efficient catalyst in the multicomponent Hantzsch reaction to make polyhydroquinolines in a way that was environmentally friendly.

2. EXPERIMENTAL SECTION

2.1. Typical Procedure for the Synthesis of MIL-101(Cr)@EDTA−Zn(II) Complex. In a typical procedure, MIL-101(Cr)−NH_2 was primarily prepared applying the hydrothermal method. In this sense, a mixture of $Cr(NO_3)_3 \cdot 9H_2O$ (2 mmol, 0.8 g), 2-aminoterephthalic acid (2 mmol, 0.360 g), and 5 mmol of NaOH was added to 15 mL of DMF. Afterward, we aimed at placing the reaction vessel under ultrasound radiation for 5 min in the ultrasound bath, and then, it was transferred to the steel autoclave reactor. Finally, it was placed in the oven at 120 °C for 24 h. After completion of the reaction and gradual cooling of the reactor, the settled green sediment was filtered with a Büchner funnel and well washed with DMF and ethanol under vacuum filtration, and then, the obtained MIL-101(Cr)−NH_2 powder was dried in an

https://doi.org/10.1021/acsomega.4c01117
ACS Omega 2024, 9, 28114−28128

Scheme 2. Synthesis of Polyhydroquinolines over the Catalysis of MIL-101(Cr)@EDTA−Zn(II) Complex

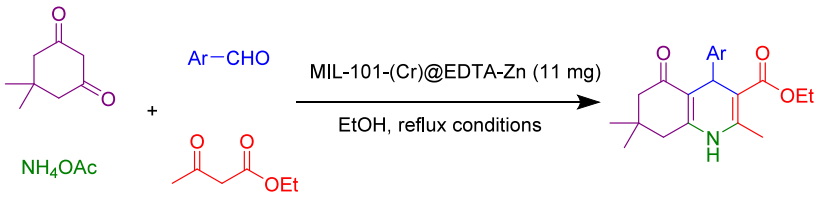

oven at 50 °C for 24 h. Moreover, the EDTA ligand was linked to MIL-101(Cr)−NH_2 through an aminolysis process. Considering this procedure, 1 g of the prepared MIL-101(Cr)−NH_2 powder was well dispersed in ethanol (50 mL), and then, 20 mL of the ethanolic solution (containing 1.2 g (4 mmol) of EDTA ligand) was injected to the MIL-101(Cr)−NH_2 suspension in a dropwise manner. Afterward, the resultant mixture was continuously mixed on a magnetic stirrer for 24 h at reflux conditions. Subsequently, the product was filtered with a Büchner funnel and then thoroughly washed using ethanol under vacuum filtration before being dried overnight in an oven at 80 °C. Finally, 10 mL of an ethanolic solution of $Zn(OAc)_2$ (0.95 g) was added to a 250 mL flask containing 100 mL of the well-dispersed ethanolic suspension of MIL-101(Cr)@EDTA (1 g), and then, the resulting mixture was subjected to continuous stirring at reflux conditions for 24 h. Subsequently, the product was filtered using a Büchner funnel and washed with water and ethanol under vacuum filtration. Moreover, the obtained MIL-101(Cr)@EDTA−Zn(II) complex was dried in an oven at 80 °C for an entire night (Scheme 1).

2.2. General Procedure for the Synthesis of Polyhydroquinolines over the Catalysis of MIL-101(Cr)@EDTA−Zn(II) Complex. A mixture of ethyl acetoacetate (1 mmol), dimedone (1 mmol), ammonium acetate (1.5 mmol), aryl aldehyde (1 mmol), and MIL-101(Cr)@EDTA−Zn(II) complex (11 mg) was stirred in ethanol (2 mL) at reflux temperature for an adequate time. After completion of the reaction (as determined using TLC), the reaction was diluted via 10 mL of hot ethanol, and then, MIL-101(Cr)@EDTA−Zn(II) catalyst was separated via simple filtration. Additionally, it was washed using ethanol and acetone, dried at 80 °C for 4 h, and then utilized in the next run. In the next step, the volume of the solvent was reduced via evaporation and the product was recrystallized from ethanol, which was then purified through washing with diethyl ether (Scheme 2).

3. RESULT AND DISCUSSION

3.1. Catalyst Characterization. Figure 1 shows the infrared spectra of the samples at each step of the synthesis process. These spectra are labeled as follows: (Figure 1a) MIL-101(Cr), (Figure 1b) MIL-101(Cr)@EDTA, and (Figure 1c) MIL-101(Cr)@EDTA−Zn(II). At the 772, 867, 975, and 1008 cm^{-1} frequencies, the stretch vibrations of the Cr−O bonds were detected. The bands at 1400 and 1614 cm^{-1} are assigned to the symmetric vibrations of the carboxylate groups and adsorbed water.[41] Regarding MIL-101(Cr)@EDTA, the appearance of strong signals from the C═O bands—in addition to N−H bands as strong signals—demonstrated the successful immobilization of EDTA through the aminolysis reaction. Finally, the observed shifts on the carboxylate and amide bands to lower frequencies that are due to the π-back-bonding effect provide conclusive evidence that the target MIL-101(Cr)@EDTA−Zn(II) complex is effective.[42−44]

Figure 2 a−d shows the XRD patterns of MIL-101(Cr)−NH_2 synthesized at a temperature range of 100−150 °C. As shown in Figure 2, the temperature was an important factor in forming the target MOF crystals. When the reaction was performed at 100 °C, an amorphous phase of MIL-101(Cr)−NH_2 was obtained. Regarding the temperature increase to 120 °C, the crystallinity of the product also increased, and sharp diffraction peaks appeared at 26.44°, 29.44°, 31.84°, 35.79°, and 39.09°. But, at higher temperatures (140 and 150 °C), the crystallinity decreased. The possible reason is that varying the temperature affects the vapor pressure in the sealed container. Moreover, at higher pressures, the MOF topology is conserved or reconstructive due to pressure-induced amorphization, leading to a phase transition and the loss of crystallinity. Interaction between an MOF and the pressure-transmitting medium can lead to spurious behavior such as negative volume compressibility. Therefore, 120 °C was selected as the optimal temperature for the synthesis of MIL-101(Cr)−NH_2. Figure 2e and 2f shows the XRD patterns for MIL-101(Cr)@EDTA−Zn(II) at a low angle and a normal angle, respectively. The PXRD pattern of MIL-101(Cr)@EDTA−Zn(II) shows additional characteristic peaks at 2θ = 12.19°, 13.99°, 15.75°, 17.20°, 18.40°, 18.71°, 20.98°, 22.99°, 24.01°, 24.61°, 25.55°, and 42.95°, which correspond to the (011), (012), (110), (111), (112), (013), (004), (014), (022), (120), (114), and (035) Miller indices (*hkl*) of the peaks (ref. code 96-411-2213).[45] In addition, comparison of the XRD patterns of MIL-101(Cr)@EDTA−Zn(II) (Figure 2f) and MIL-101(Cr)−NH_2 (Figure 2c) shows that after the PSM process, several new peaks appeared in the catalyst pattern. These new peaks are the characteristic diffraction peaks of the EDTA−Zn complex, which prove that the target complex was successfully immobilized on the MOF support. Furthermore, the similarity of the main PXRD diffraction peaks of the catalyst and MIL-101(Cr)−NH_2 shows that the crystalline phase of the support did not change during the PSM process.

Figure 3 shows the MIL-101(Cr)@EDTA−Zn(II) complex TGA and DSC curves. The initial mass loss (12%) below 200 °C is due to the evaporation of moisture absorbed in the pores of MOF from solvents and air.[2,46] The next weight loss that occurred in the range of 225−480 °C, which is equal to 45.02%, was caused by the pyrolysis of the organic moieties.[2,46,47] The DSC curve shows two continuous endothermic pyrolysis processes for this range that confirm the stepwise pyrolysis of 2-aminoterephthalic acid and EDTA in the MOF-supported complex. In addition, there was still 37% of the material, even after heating to 1000 °C, which is almost the same as the approximate quantity of zinc and chromium that was determined using EDX. The observed results confirm the formation of MIL-101(Cr)−NH_2 and its stepwise functionalization via an EDTA−Zn(II) complex.

https://doi.org/10.1021/acsomega.4c01117
ACS Omega 2024, 9, 28114−28128

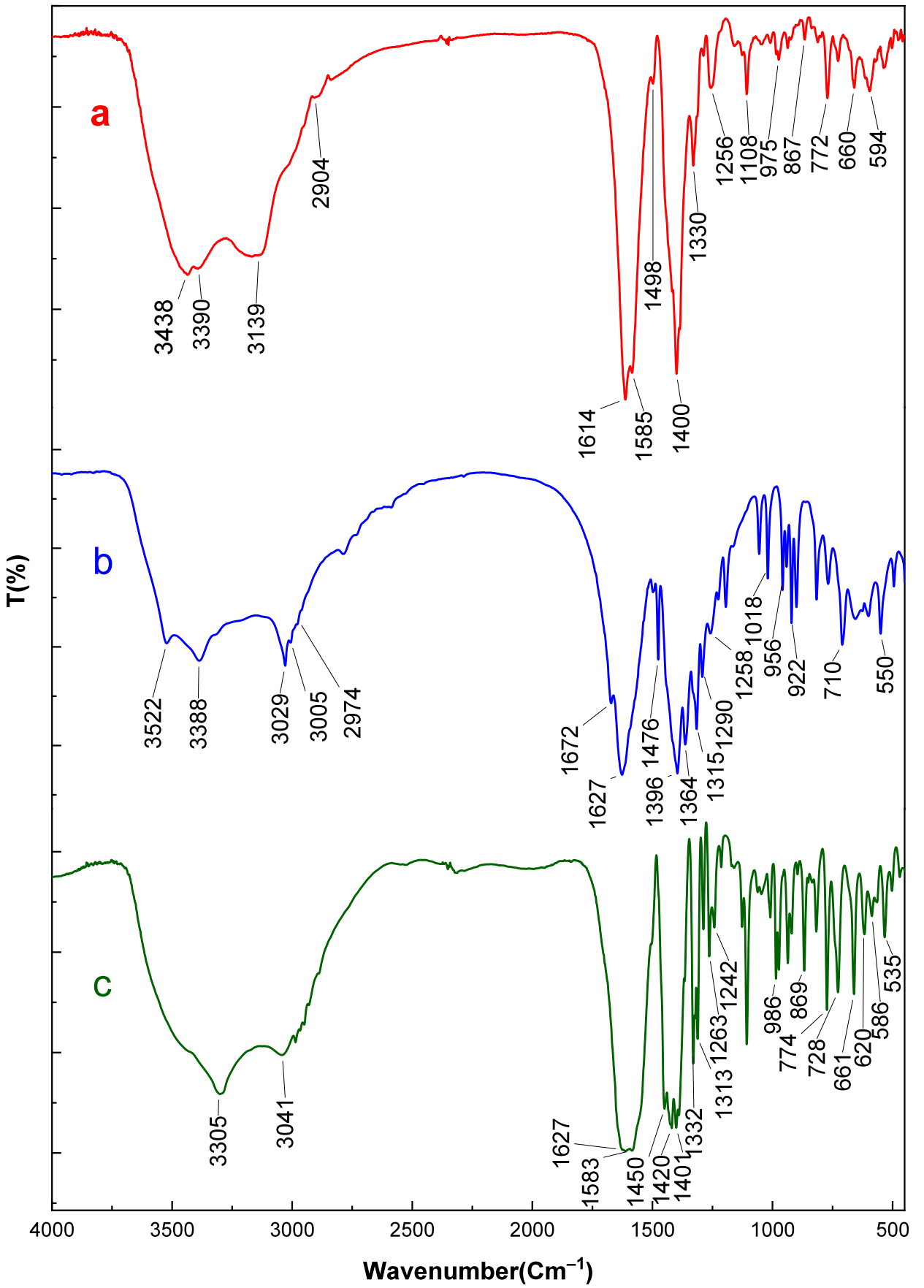

Figure 1. FT-IR analysis of (a) MIL-101(Cr)−NH_2, (b) MIL-101(Cr)@EDTA, and (c) MIL-101(Cr)@EDTA−Zn(II) complexes.

https://doi.org/10.1021/acsomega.4c01117
ACS Omega 2024, 9, 28114−28128

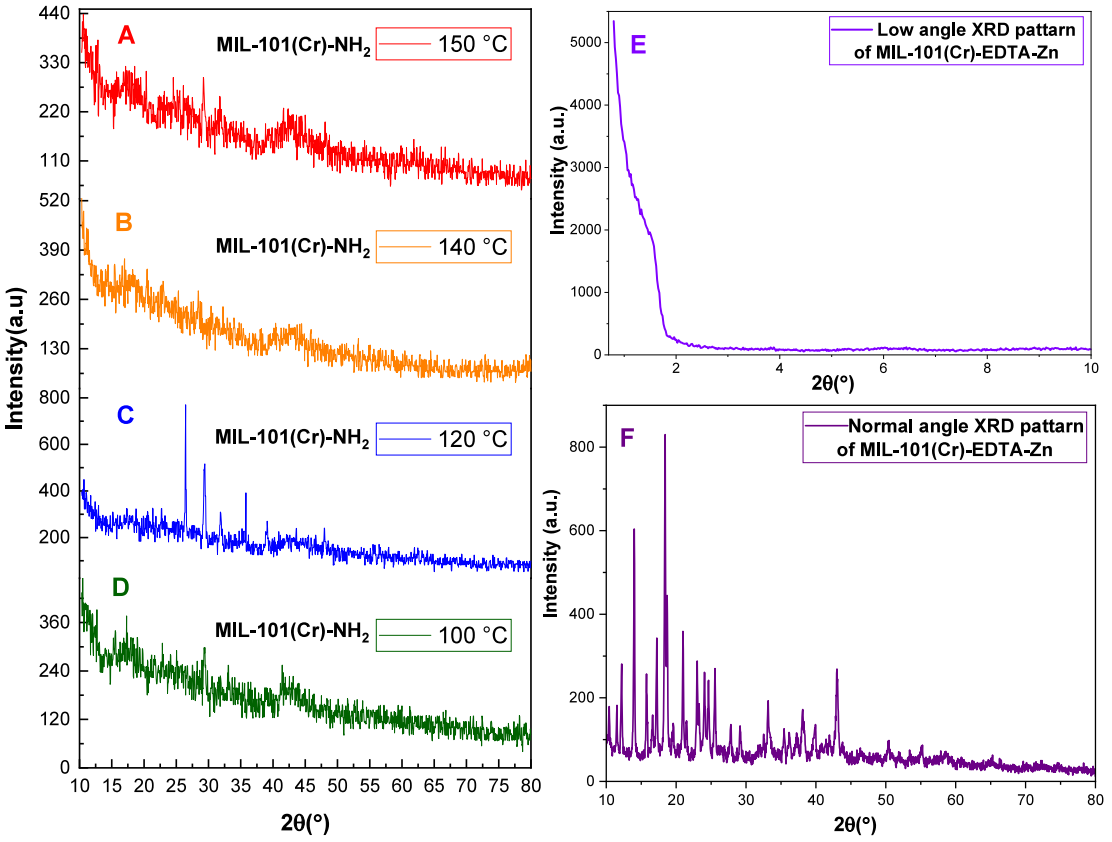

Figure 2. XRD patterns of MIL-101(Cr)−NH_2 synthesized at (a) 150, (b) 140, (c) 120, (d) 100, and 150 °C and (e) low-angle and (f) normal-angle MIL-101(Cr)@EDTA−Zn(II) complex.

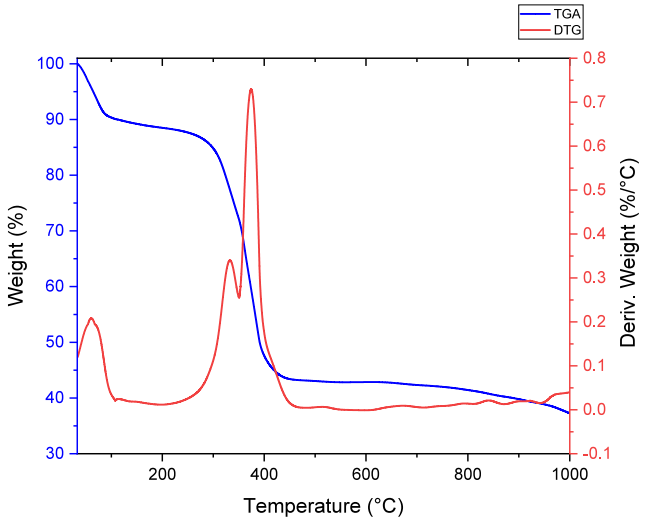

Figure 3. TGA and DSC curves of MIL-101(Cr)@EDTA−Zn(II) complex.

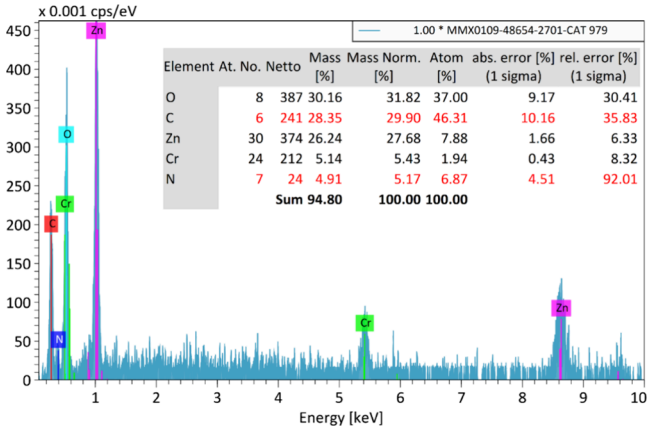

Figure 4. EDX analysis of MIL-101(Cr)@EDTA−Zn(II) complex.

EDX spectroscopy shows that the MIL-101(Cr)@EDTA−Zn(II) complex has the expected components, which is in line with the goal of our strategy for making the heterogenized Zn complex (Figure 4). Regarding this spectrum, the existence of Cr is related to the metal oxide clusters of MOF support. Organic ligands are responsible for the presence of large amounts of C, N, and O elements. Moreover, the existence of the Zn element shows the successful complexation of MIL-101(Cr)@EDTA with the Zn ions. Finally, based on ICP-OES analysis, the exact amounts of Cr and Zn elements in the sample were 0.54×10^{-3} and 1.86×10^{-3} mol·g^{-1}, respectively, confirming the complexation of metal ions with the ligand.

STEM elemental mapping shows that the Cr, C, N, O, and Zn elements are homogeneously spread out in the MIL-101(Cr)@EDTA−Zn(II) matrix (Figure 5). This shows that EDTA−Zn(II) is uniformly grown on the MIL-101(Cr)−NH_2 MOF. Moreover, it can be seen that the high content of Zn in the sample, which is close to the EDX and ICP values, proves the successful formation of the target complex with good accessibility of Zn sites for catalytic applications.

SEM was used to study the surface morphology of MIL-101(Cr)@EDTA−Zn(II) (Figure 6). The SEM pictures show the formation of nanosheet-structure MOF crystals with a

https://doi.org/10.1021/acsomega.4c01117
ACS Omega 2024, 9, 28114−28128

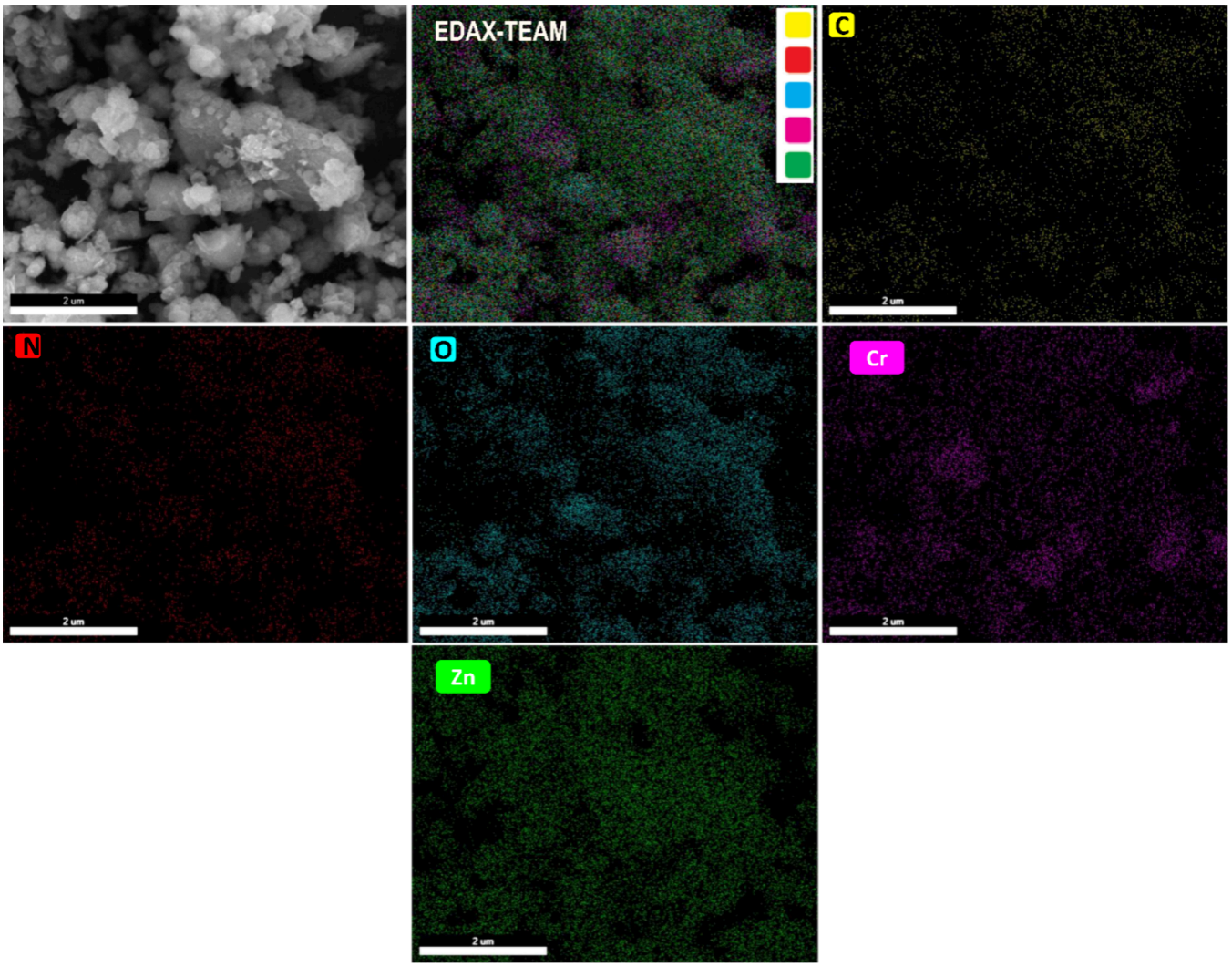

Figure 5. STEM elemental mapping images of MIL-101(Cr)@EDTA−Zn(II) complex.

hexagonal shape that are in close contact with a uniformly distributed layer with cauliflower-like morphology and homogeneous size around them. Because the EDTA−Zn(II) complex is bulky and covalently supported to MIL-101(Cr)−NH_2, catalytic functionality loading should affect the nanomorphology of the MOF. Significantly, the observations confirm that the chemical modifications affected the morphology of the parent MOF. However, the initial morphology was retained in some areas, indicating that the prepared catalyst has good quality in terms of crystallinity and its components which have formed chemical bonds rather than simple physical mixing.

To delve into the morphology and particle size of the MIL-101(Cr)@EDTA−Zn(II) complex, we conducted TEM examinations (Figure 7). The transmission electron micrographs unveil the crystalline nature of the MIL-101(Cr)@EDTA−Zn(II) complex particles. Notably, the stepwise modification and functionalization of the MOF surface seem to influence the catalytic support, introducing certain variations. Despite these effects, the synthesized MOF exhibits distinctive characteristics indicative of its crystalline structure. An interesting observation from the micrographs is the discernible space between the MIL-101(Cr) support and the catalytic shell. This spatial distinction provides compelling evidence supporting the assertion that the MIL-101(Cr) support indeed takes the form of a solid crystal. This nuanced understanding of the complex's structural features contributes to a more comprehensive characterization of its morphology, shedding light on the interplay between the catalytic components and the MOF support.

The N_2 adsorption and desorption isotherms were used to characterize the porosity of MIL-101(Cr)@EDTA−Zn(II). As depicted in Figure 8, the absorption isotherm of type III and a hysteresis loop of type H3 are evident, characteristics classified by IUPAC as indicative of mesoporous materials. Table 1 provides details about the synthetic sample.[48] The results are presented in Table 1. The obtained results reveal that the surface area and pore volume of the MIL-101(Cr)@EDTA−Zn(II) complex are 91.259 m^2/g and 0.2589 cm^3/g, respectively. These values demonstrate a notable decrease compared to MIL-101(Cr)−NH_2,[48] confirming the successful postmodification

3.2. Catalytic Study. Our studies on the synthesis of polyhydroquinolines began with the reaction of 4-chlorobenzaldehyde as the model substrate. Primarily, the effect of the solvent was looked into, and then, the performance of the reaction was tested with common laboratory solvents that are in line with green chemistry using a random and fixed amount

https://doi.org/10.1021/acsomega.4c01117
ACS Omega 2024, 9, 28114−28128

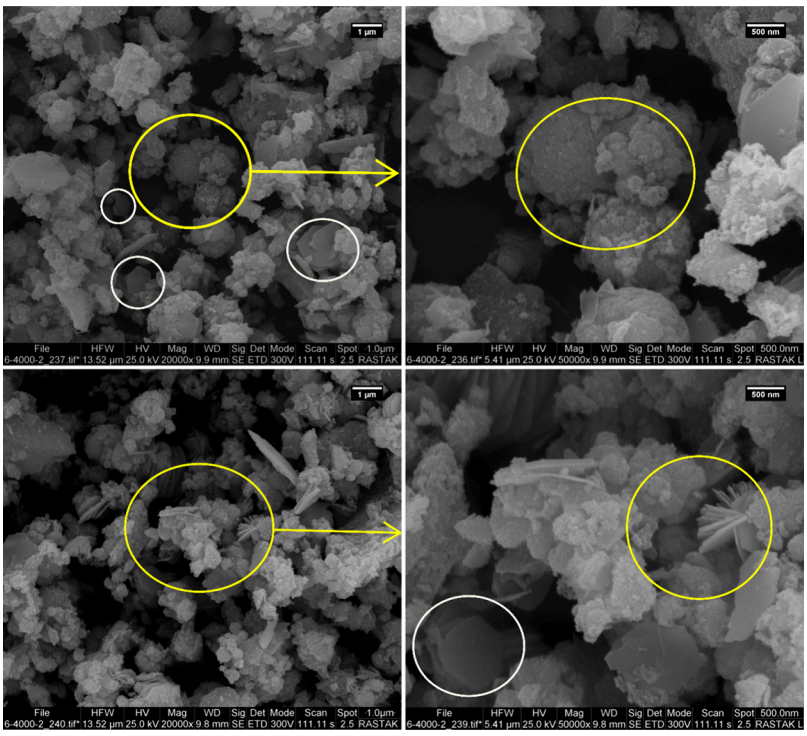

Figure 6. SEM images of MIL-101(Cr)@EDTA−Zn(II) complex.

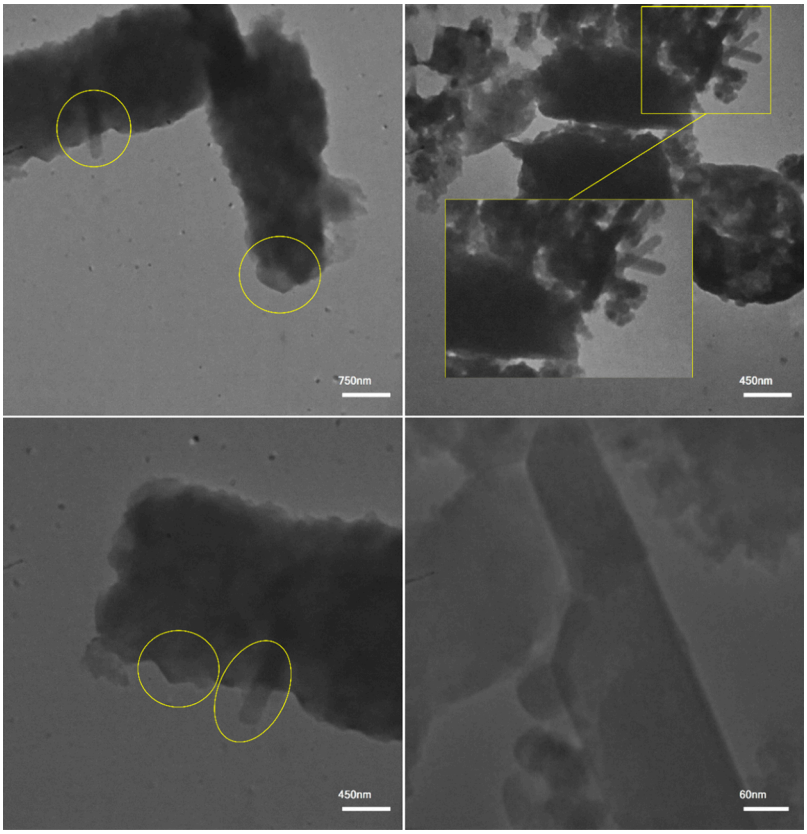

Figure 7. TEM images of MIL-101(Cr)@EDTA−Zn(II) complex.

of catalyst (5 mg) (Table 2, entries 1−6). The results showed that both acetonitrile and dimethylformamide are good solvents for these organic transformations. On the contrary, there are problems in using these solvents, i.e., the need for more purification steps and the need to use ethyl acetate for extraction in a separating funnel, making this method less effective and less cost effective. When the reaction was tested in water, the yield of the corresponding product went down.

https://doi.org/10.1021/acsomega.4c01117
ACS Omega 2024, 9, 28114−28128

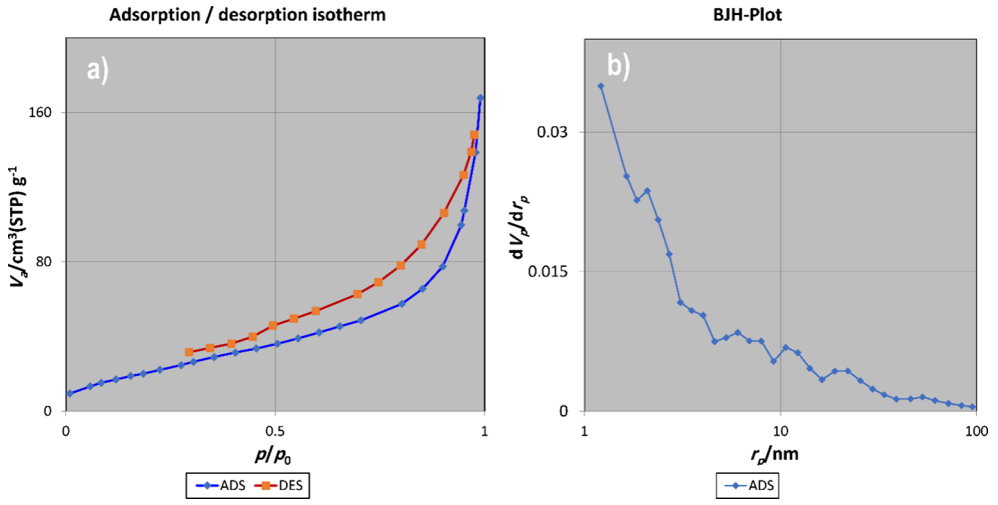

Figure 8. N_2 adsorption and desorption isotherms and pore size distribution curve of MIL-101(Cr)@EDTA−$Zn^{(II)}$.

Table 1. BET Characteristics of MIL-101(Cr)@EDTA−Zn(II)

sample	BET surface area (m^2/g)	average pore diameter (nm)	total pore volume (cm^3/g)
MIL-101(Cr)−NH_2[48]	1708	<10	1.46
MIL-101(Cr)@EDTA−$Zn^{(II)}$	91.259	11.346	0.2589

This is likely because some of the raw materials did not dissolve and there were fewer collisions and interactions between the raw materials, which are needed to turn them into intermediates and the corresponding products. The results show that ethanol gives the best yield, and accordingly, it was chosen as the best medium for this reaction (Tables 2, entry 4).

Considering ethanol as the optimal solvent, the effect of the catalyst amount was looked at as the second optimization parameter. At the outset of the catalyst optimization studies, an uncatalyzed reaction was performed without adding any MIL-101(Cr)@EDTA−Zn(II) or additive, which resulted in trace product formation (Table 2, entry 7). The next step involved

Table 2. Optimization of the Reaction Conditions for the Synthesis of Polyhydroquinolines over the Catalysis of MIL-101(Cr)@EDTA−Zn(II)

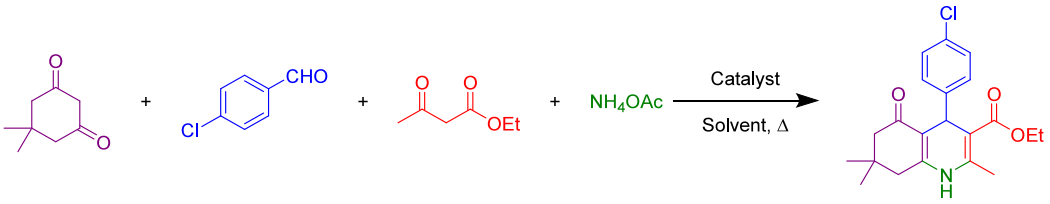

entry	catalyst	amount catalyst (mg)	solvent	temperature (°C)	time (min)	yield (%)[a,b]
1	MIL-101(Cr)@EDTA−Zn(II)	5	DI water	80	15	43
2	MIL-101(Cr)@EDTA−Zn(II)	5	CH_3CN	80	15	85
3	MIL-101(Cr)@EDTA−Zn(II)	5	DMSO	80	15	55
4	MIL-101(Cr)@EDTA−Zn(II)	5	EtOH	reflux	15	64
5	MIL-101(Cr)@EDTA−Zn(II)	5	MeOH	reflux	15	60
6	MIL-101(Cr)@EDTA−Zn(II)	5	solvent free	80	15	47
7	catalyst free		EtOH	reflux	60	trace
8	MIL-101(Cr)@EDTA−Zn(II)	3	EtOH	reflux	15	51
9	MIL-101(Cr)@EDTA−Zn(II)	6	EtOH	reflux	15	82
10	MIL-101(Cr)@EDTA−Zn(II)	8	EtOH	reflux	15	91
11	MIL-101(Cr)@EDTA−Zn(II)	11	EtOH	reflux	15	98
12	MIL-101(Cr)@EDTA−Zn(II)	15	EtOH	reflux	15	98
13	MIL-101(Cr)@EDTA−Zn(II)	11	EtOH	25	15	trace
14	MIL-101(Cr)@EDTA−Zn(II)	11	EtOH	50	15	63
15	MIL-101(Cr)@EDTA−Zn(II)	11	EtOH	60	15	84
16	MIL-101(Cr)	11	EtOH	reflux	15	47
17	MIL-101(Cr)@EDTA	11	EtOH	reflux	15	53
18	EDTA−$Zn^{(II)}$	11	EtOH	reflux	15	72

[a]Isolated yield. [b]Reaction conditions: 4-Chlorobenzaldehyde (1 mmol), dimedone (1 mmol), ethyl acetoacetate (1 mmol), ammonium acetate (1.5 mmol), catalyst (mg), and solvent (3 mL).

https://doi.org/10.1021/acsomega.4c01117
ACS Omega 2024, 9, 28114−28128

Table 3. Synthesis of Polyhydroquinoline Derivatives over the Catalysis of MIL-101(Cr)@EDTA−Zn(II) Complex[4961]

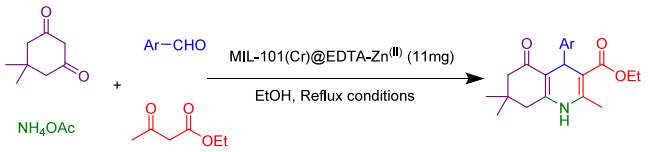

Entry	Aryl aldehyde	Product	Time (min)	Yield (%)[a,b]	TON	TOF	Melting point measured	Melting point literature
1		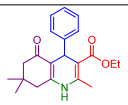	25	97	102.10	245	201–202	200–203 [49]
2		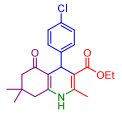	15	98	103.15	412	241–244	242–245 [49]
3		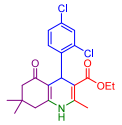	60	88	92.63	92	217–218	218–219 [50]
4		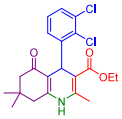	110	83	87.36	47.65	226–228	227–229 [51]
5		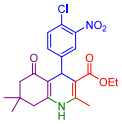	35	91	95.78	164.21	220–222	220–222 [52]
6		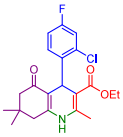	90	85	89.47	59.64	180–181	180–181 [50]
7		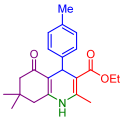	30	94	98.94	197.89	194–195	192–193 [49]
8		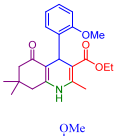	45	91	95.78	127.71	249–251	250–253 [53]
9		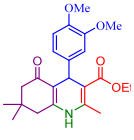	60	88	92.63	92	199–201	200–201 [54]
10		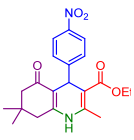	10	98	103.15	618	234–236	235–237 [49]
11		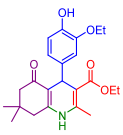	95	89	93.68	59.16	197–199	198–200 [55]
12		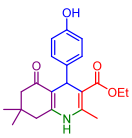	90	91	95.78	63.85	225–228	225–227 [49]
13		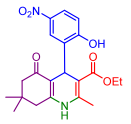	35	92	96.84	166	229–230	229–230 [56]
14		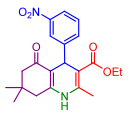	25	92	96.84	232.42	228–229	228–229 [57]
15		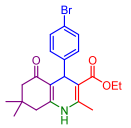	20	95	100	300	249–252	248–250 [49]
16		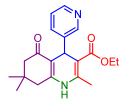	40	94	98.94	148.42	230–233	232–235 [49]
17		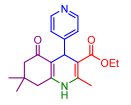	35	95	100	171.42	218–220	218–220 [58]
18		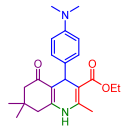	50	93	97.89	117.47	234–237	234–236 [59]
19		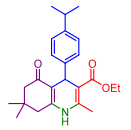	35	91	95.78	164.21	182–184	181–183 [54]
20			75	87	91.57	73.26	232–233	232–234 [60]
21			40	93	97.89	146.84	298–300	298–300 [53]
22			100	84	88.42	53.05	305–307	305–307 [61]

[a]Isolated yield. [b]Reaction conditions: Aromatic aldehyde (1 mmol), dimedone (1 mmol), ethyl acetoacetate (1 mmol), ammonium acetate (1.5 mmol), and MIL-101(Cr)@EDTA−Zn(II) (11 mg) in ethanol (2 mL) under reflux conditions.

https://doi.org/10.1021/acsomega.4c01117
ACS Omega 2024, 9, 28114−28128

Scheme 3. Possible Mechanism for Hantzsch Reaction over the Catalysis of MIL-101(Cr)@EDTA−Zn(II) Complex

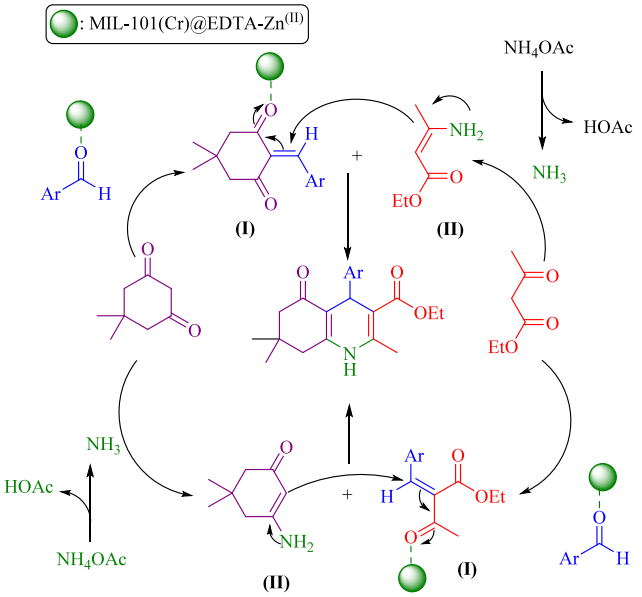

Figure 9. Reusability of MIL-101(Cr)@EDTA−Zn(II) complex in Hantzsch reaction.

adding different amounts of MIL-101(Cr)@EDTA−Zn(II) to the reaction mixture as catalyst and also evaluating their efficiency and effect on the reaction progress (Table 2, entries 8−12). The results show that the reaction worked better when the amount of catalyst went from 3 to 11 mg. Based on this evaluation, 11 mg of the catalytic complex gave the best results (98% efficiency). In addition, increasing the catalyst loading (15 mg) did not lead to a yield increment as compared to the amount of 11 mg. Because of this, 11 mg of the MIL-101(Cr)@EDTA−Zn(II) complex was thought to be the best amount of the catalyst for this reaction.

In order to find the best temperature for the reaction, the effects of different temperatures, from room temperature to the reflux temperature, were studied. The results, which are shown in Table 2, show that only a trace amount of the product was formed at room temperature. On the other hand, as the temperature goes up, the reaction proceeds faster. Significantly, the best results were found at reflux conditions. Finally, we

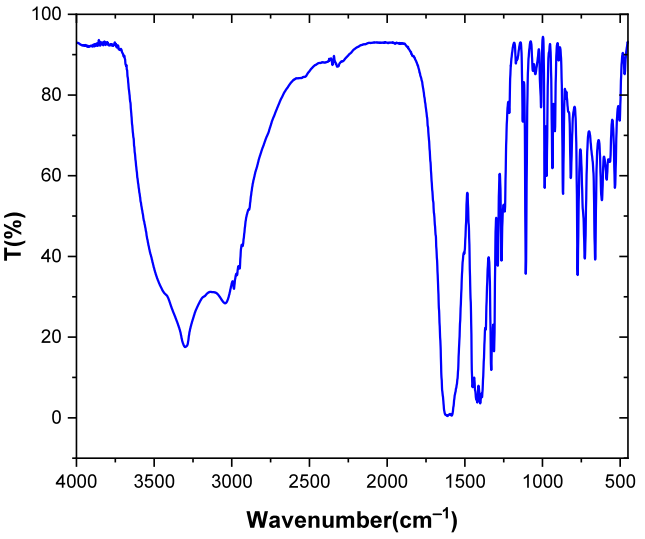

Figure 10. FT-IR analysis of recovered MIL-101(Cr)@EDTA−Zn(II) catalyst.

investigated the impact of catalyst moieties on the reaction (Table 2, entries 16−18). The results indicate that lower performance was observed with compounds containing such moieties; these blank testes indicate synergistic effects between the MOFs and the complex. Conversely, the MIL-101(Cr)@EDTA−Zn(II) catalyst demonstrated superior performance, yielding the best overall yield (Table 2, entry 11). As a result, the reflux temperature was considered the optimal temperature. According to the obtained results, the optimal conditions include an amount of 11 mg of the MIL-101(Cr)@EDTA−Zn(II) catalyst in ethanol under reflux conditions.

After figuring out the best conditions for the synthesis of polyhydroquinolines, the developed method was examined in the synthesis of different derivatives of these heterocyclic compounds. This was done to test the milestones and limits of the method. The effect of electron-donating and electron-drawing groups on different positions of the aryl ring on the yield and reaction time was studied. The results are summarized in Table 3. The results show that the studied substrates were turned into polyhydroquinoline derivatives in a short amount of time and with good to excellent yields. This illustrates that the proposed method to make these compounds works well. Moreover, the reaction of aryl aldehydes with positive resonance affects on the aryl ring (electron-donating groups (Me, OMe)) reacted in a longer time. The efficiency of these organic changes was average during this reaction. This is likely due to the transfer of an electron to the carbon of the carbonyl group, which has a partial positive charge, leading to the stabilization of this carbon and making that group less reactive. On the other hand, aldehydes bearing functionalities with a negative resonance effect in the ortho and para positions of the aromatic ring reacted faster and more efficiently. The main reason for this big difference is that the positive charge on the carbon of the functional group of the aldehyde increased, which made this group more active.

Based on what we had learned before, a plausible reaction mechanism (Scheme 3) was proposed for this transformation (Scheme 3).[62,63] The Lewis acid sites including Zn and Cr will initially lead to the aryl aldehyde activation. Afterward, the

https://doi.org/10.1021/acsomega.4c01117
ACS Omega 2024, 9, 28114−28128

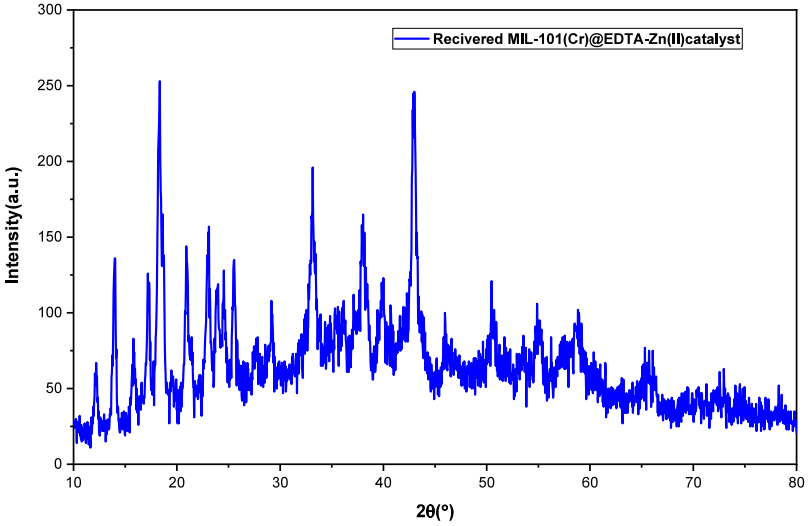

Figure 11. XRD pattern of recovered MIL-101(Cr)@EDTA−Zn(II) catalyst.

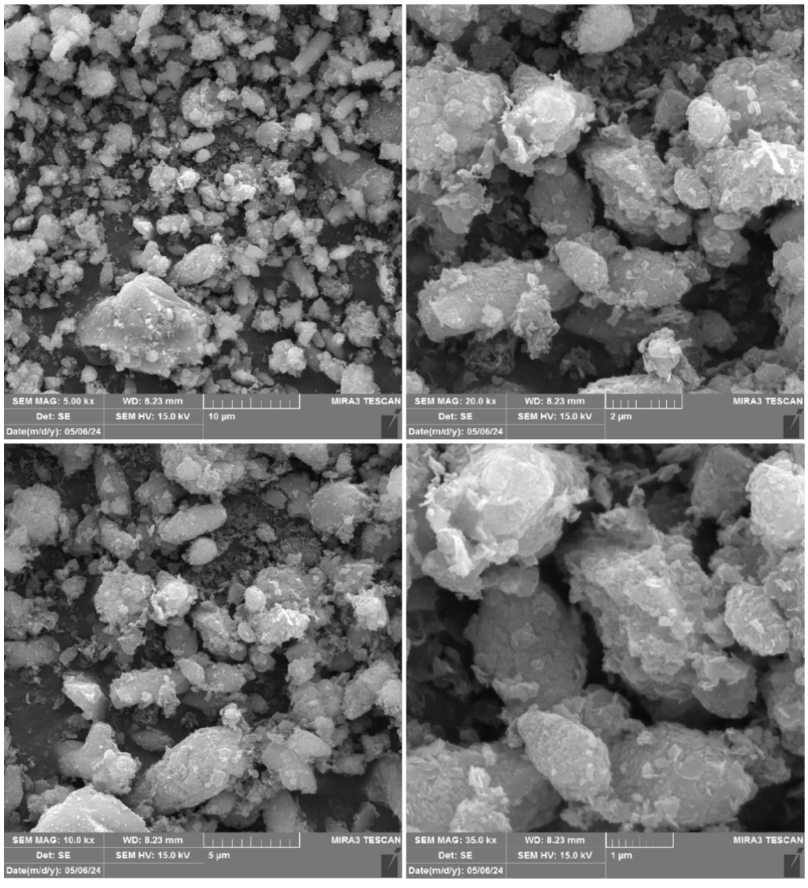

Figure 12. XRD pattern of recovered MIL-101(Cr)@EDTA−Zn(II) catalyst.

amine sites in the catalyst remove a proton from the active methylene compounds to produce a carbanion. Subsequently, this carbanion rapidly interacts with the activated aryl aldehyde to produce the Knoevenagel intermediate (I), which requires the removal of water molecules and the renewal of the metal complexes. In contrast, the combination of ethyl acetoacetate and ammonium acetate will result in the formation of an enaminone molecule. Moreover, the mesylate anion removes the proton from the enaminone (II), and then, the resulting anion combines with the adduct (I) to form polyhydroquinolines. This process also results in eliminating water molecules and renewing the catalyst.

3.3. Recovery and Reusability. One thing that heterogeneous catalysts have in common is that they can be recycled and reused again. This is important in both industry and the lab considering economic and environmental issues. The MIL-101(Cr)@EDTA−Zn(II) complex capacity in being recycled and reused in the above-mentioned model reaction was evaluated. As seen in Figure 9, the catalyst was recovered and employed for eight continuous runs. Evaluation revealed

https://doi.org/10.1021/acsomega.4c01117
ACS Omega 2024, 9, 28114−28128

Table 4. Comparison of Catalytic Efficiency of MIL-101(Cr)@EDTA−Zn(II) Complex in Model Reactions

entry	catalyst	conditions	time (min)	yield (%)	ref
1	$FeAl_2O_4$	EtOH, reflux	180	90	63
2	$CoFe_2O_4$@Pr	EtOH, reflux	145	96	64
3	H_2PO_4−SCMNPs	solvent free, 80 °C	20	92	65
4	AIL-SCMNPs	solvent free, 60 °C	15	80	66
5	Fe_3O_4@GA@IG	EtOH, ultrasound	45	89	67
6	Zn−MOF	PEG-400, 80 °C	85	96	62
7	MIL-101(Cr)@EDTA−$Zn^{(II)}$	EtOH, reflux	15	98	this work

that there was no appreciable loss of catalytic activity at each stage, and the recovered catalytic complex still possessed unique catalytic properties. The recovered catalyst underwent thorough characterization via ICP-OES analysis, confirming the presence of Cr (10.6 wt %) and Zn (13.4 wt %), consistent with their concentrations in the fresh catalyst. Additionally, FT-IR and XRD analyses of the recycled catalyst exhibited remarkable consistency with the spectrum of the fresh catalyst (Figures 10 and 11). This comprehensive characterization provides compelling evidence for the stability of both the crystalline phase and the functional group content of the catalyst over successive reaction cycles. Moreover, SEM images indicate that the recovered catalyst has maintained its high quality in terms of crystallinity even after eight cycles (Figure 12). These findings affirm the catalyst's stability under optimal reaction conditions.

3.4. Leaching and Hot Filtration Tests. An investigation into the heterogeneous nature of the MIL-101(Cr)@EDTA−Zn(II) complex and the stability of EDTA−Zn(II) on the catalytic support was carried out through performing hot filtration and leaching tests on the model reaction according to the method that was described before in the literature.[62] The findings of the hot filtration experiment substantiated the hypotheses that the MIL-101(Cr)@EDTA−Zn(II) complex is heterogeneous in composition and that it is insoluble in the reaction medium. The ICP-OES analysis shows that there was no metal leaching into the reaction medium.

3.5. Comparison. As compared to other methods, the catalytic activity and efficiency of this protocol for the synthesis of polyhydroquinolines are depicted in Table 4. This comparison shows that the MIL-101(Cr)@EDTA−Zn(II) catalytic complex is an efficient catalyst for the synthesis of these compounds. Moreover, it also shows that our protocol is superior in terms of the amount of time required for the reaction, the temperature of the reaction, and the expected yield for both of the aryl aldehydes with steric hindrance and positive and negative resonance effects.

4. CONCLUSION

In summary, PSM was used as a simple and easy method to synthesize the EDTA−Zn(II) complex that was immobilized on the MIL-101(Cr)−NH_2 MOF as a porous substrate. The constructed catalytic complex was very good at producing polyhydroquinoline derivatives through Hantzsch reaction in an environmentally friendly way. Comparison of its activity to other catalytic systems showed that this method is better from both efficiency and recycling points of view. Moreover, this catalytic system has a lot of benefits, such as how cheap it is to be made, how different it is, how stable it is physically and chemically, and how easy it is to be recycled without losing much of its effectiveness.

■ ASSOCIATED CONTENT

Data Availability Statement

The data that support the findings of this study are available in the Supporting Information of this article.

Supporting Information

The Supporting Information is available free of charge at https://pubs.acs.org/doi/10.1021/acsomega.4c01117.

Detailed synthetic procedures, and copies of ^{1}H NMR and ^{13}C NMR spectra (DOCX)

■ AUTHOR INFORMATION

Corresponding Authors

Ahmad Nikseresht − *Department of Chemistry, Payame Noor University, 19395-4697 Tehran, Iran;* orcid.org/0000-0002-4342-8782; Phone: +98-918-8418754; Email: a_nik55@yahoo.com, ahmad.nikseresht@pnu.ac.ir

Masoud Mohammadi − *Department of Chemistry, Faculty of Science, Ilam University, 69315-516 Ilam, Iran;* orcid.org/0000-0002-1043-3470; Phone: +98918682610; Email: tbr.masoud@gmail.com

Author

Fatemeh Ghoochi − *Department of Chemistry, Payame Noor University, 19395-4697 Tehran, Iran*

Complete contact information is available at: https://pubs.acs.org/10.1021/acsomega.4c01117

Author Contributions

Ahmad Nikseresht: Supervision, conceptualization, review, and editing of the final version and submitting the manuscript for publication. **Fatemeh Ghoochi**: Performed most of the practical laboratory work as part of her master's thesis supervised by Ahmad Nikseresht. **Masoud Mohammadi**: Contributed to conceptualization, practical laboratory work, software, writing, review, and editing of the manuscript draft.

Notes

The authors declare no competing financial interest.

■ ACKNOWLEDGMENTS

This work was financially supported by the Payame Noor University, Tehran, Iran.

■ REFERENCES

(1) Tombesi, A.; Pettinari, C. Metal Organic Frameworks as Heterogeneous Catalysts in Olefin Epoxidation and Carbon Dioxide Cycloaddition. *Inorganics* **2021**, *9* (11), 81.

(2) Ghobakhloo, F.; Mohammadi, M.; Ghaemi, M.; Azarifar, D. Post-Synthetic Generation of Amino-Acid-Functionalized UiO-66-NH 2 Metal-Organic Framework Nanostructures as an Amphoteric Catalyst for Organic Reactions. *ACS Appl. Nano Mater.* **2024**, *7* (1), 1265−1277.

(3) Sanati, S.; Morsali, A.; García, H. Metal-Organic Framework-Based Materials as Key Components in Electrocatalytic Oxidation and Reduction Reactions. *J. Energy Chem.* **2023**, *87*, 540−567.
(4) Chung, W.-T.; Mekhemer, I. M. A.; Mohamed, M. G.; Elewa, A. M.; EL-Mahdy, A. F. M.; Chou, H.-H.; Kuo, S.-W.; Wu, K. C.-W. Recent Advances in Metal/covalent Organic Frameworks Based Materials: Their Synthesis, Structure Design and Potential Applications for Hydrogen Production. *Coord. Chem. Rev.* **2023**, *483*, 215066.
(5) Hussain-Khil, N.; Ghorbani-Choghamarani, A.; Mohammadi, M. A New Silver Coordination Polymer Based on 4,6-Diamino-2-Pyrimidinethiol: Synthesis, Characterization and Catalytic Application in Asymmetric Hantzsch Synthesis of Polyhydroquinolines. *Sci. Rep.* **2021**, *11* (1), 15657.
(6) Li, Y.; Wu, Y.; Liu, K.; Delbari, S. A.; Kim, A.; Sabahi Namini, A.; Le, Q. V.; Shokouhimehr, M.; Xia, C.; Jang, H. W.; Varma, R. S.; Luque, R. Metal-Organic Framework-Based Nanostructured Catalysts: Applications in Biomass Conversion. *Fuel* **2023**, *340*, 127482.
(7) Andrade, L. S.; Lima, H. H. L. B.; Silva, C. T. P.; Amorim, W. L. N.; Poço, J. G. R.; López-Castillo, A.; Kirillova, M. V.; Carvalho, W. A.; Kirillov, A. M.; Mandelli, D. Metal-organic Frameworks as Catalysts and Biocatalysts for Methane Oxidation: The Current State of the Art. *Coord. Chem. Rev.* **2023**, *481*, 215042.
(8) Nikseresht, A.; Bagherinia, R.; Mohammadi, M.; Mehravar, R. Phosphomolybdic Acid Hydrate Encapsulated in MIL-53 (Fe): A Novel Heterogeneous Heteropoly Acid Catalyst for Ultrasound-Assisted Regioselective Nitration of Phenols. *RSC Adv.* **2022**, *13* (1), 674−687.
(9) Abazari, R.; Sanati, S.; Bajaber, M. A.; Javed, M. S.; Junk, P. C.; Nanjundan, A. K.; Qian, J.; Dubal, D. P. Design and Advanced Manufacturing of NU-1000 Metal-Organic Frameworks with Future Perspectives for Environmental and Renewable Energy Applications. *Small* **2024**, *20* (15), 2306353.
(10) Pan, Y.; Sanati, S.; Abazari, R.; Noveiri, V. N.; Gao, J.; Kirillov, A. M. Pillared-MOF@NiV-LDH Composite as a Remarkable Electrocatalyst for Water Oxidation. *Inorg. Chem.* **2022**, *61* (51), 20913−20922.
(11) Panda, J.; Sahoo, T.; Swain, J.; Panda, P. K.; Tripathy, B. C.; Samantaray, R.; Sahu, R. The Journey from Porous Materials to Metal-Organic Frameworks and Their Catalytic Applications: A Review. *Curr. Org. Synth.* **2023**, *20* (2), 220−237.
(12) Nikseresht, A.; Mirzaei, N.; Masoumi, S.; Azizi, H. R. Response Surface Methodology Optimization of Friedel-Crafts Acylation Using Phosphotungstic Acid Encapsulation in a Flexible Nanoporous Material. *ACS Mater. Au* **2023**, *3*, 123.
(13) Nikseresht, A.; Aderang, E. Encapsulation of Phosphotungstic Acid in the Nanostructure of Metal-Organic Framework as a Heterogonous Catalyst Used for Fries Rearrangement of O-Acyloxy Benzenes in Para-Situation. *Appl. Chem. Today* **2021**, *16* (61), 25−38.
(14) Nikseresht, A.; Daniyali, A.; Ali-Mohammadi, M.; Afzalinia, A.; Mirzaie, A. Ultrasound-Assisted Biodiesel Production by a Novel Composite of Fe(III)-Based MOF and Phosphotangestic Acid as Efficient and Reusable Catalyst. *Ultrason. Sonochem.* **2017**, *37*, 203−207.
(15) Hu, Y.; Abazari, R.; Sanati, S.; Nadafan, M.; Carpenter-Warren, C. L.; Slawin, A. M. Z.; Zhou, Y.; Kirillov, A. M. A Dual-Purpose Ce(III)-Organic Framework with Amine Groups and Open Metal Sites: Third-Order Nonlinear Optical Activity and Catalytic CO 2 Fixation. *ACS Appl. Mater. Interfaces* **2023**, *15* (31), 37300−37311.
(16) Xiao, W.; Cheng, M.; Liu, Y.; Wang, J.; Zhang, G.; Wei, Z.; Li, L.; Du, L.; Wang, G.; Liu, H. Functional Metal/Carbon Composites Derived from Metal-Organic Frameworks: Insight into Structures, Properties, Performances, and Mechanisms. *ACS Catal.* **2023**, *13* (3), 1759−1790.
(17) Zhao, D.; Li, W.; Wen, R.; Lei, N.; Li, W.; Liu, X.; Zhang, X.; Fan, L. Eu(III)-Functionalized MOF-Based Dual-Emission Ratiometric Sensor Integrated with Logic Gate Operation for Efficient Detection of Hippuric Acid in Urine and Serum. *Inorg. Chem.* **2023**, *62* (6), 2715−2725.
(18) Zhao, D.; Li, W.; Wen, R.; Li, W.; Liu, X.; Zhang, X.; Fan, L. Tb(III) Functionalized MOF Based Self-Calibrating Sensor Integrated with Logic Gate Operation for Efficient Epinephrine Detection in Serum. *J. Rare Earths* **2024**, *42*, 987.
(19) Kang, D. W.; Kang, M.; Hong, C. S. Post-Synthetic Modification of Porous Materials: Superprotonic Conductivities and Membrane Applications in Fuel Cells. *J. Mater. Chem. A* **2020**, *8* (16), 7474−7494.
(20) Karami, Z.; Khodaei, M. M. Post-synthetic Modification of IR-MOF-3 as Acidic-Basic Heterogeneous Catalyst for One-Pot Synthesis of pyrimido[4,5-B]quinolones. *Res. Chem. Intermed.* **2022**, *48* (4), 1773−1792.
(21) Keypour, H.; Kouhdareh, J.; Alavinia, S.; Rabiei, K.; Mohammadi, M.; Maryamabadi, A.; Babaei, S. Post-Synthetic Modification of Dual-Porous UMCM-1-NH2 with Palladacycle Complex as an Effective Heterogeneous Catalyst in Suzuki and Heck Coupling Reactions. *J. Organomet. Chem.* **2023**, *989*, 122646.
(22) Ghobakhloo, F.; Azarifar, D.; Mohammadi, M.; Keypour, H.; Zeynali, H. Copper(II) Schiff-Base Complex Modified UiO-66-NH2(Zr) Metal-Organic Framework Catalysts for Knoevenagel Condensation-Michael Addition-Cyclization Reactions. *Inorg. Chem.* **2022**, *61* (12), 4825−4841.
(23) Ghorbani-Choghamarani, A.; Taherinia, Z.; Mohammadi, M. Facile Synthesis of Fe3O4@GlcA@Ni-MOF Composites as Environmentally Green Catalyst in Organic Reactions. *Environ. Technol. Innov.* **2021**, *24*, 102050.
(24) Zou, M.; Dong, M.; Zhao, T. Advances in Metal-Organic Frameworks MIL-101(Cr). *Int. J. Mol. Sci.* **2022**, *23* (16), 9396.
(25) Lopez-Magano, A.; Jiménez-Almarza, A.; Aleman, J.; Mas-Ballesté, R. Metal-organic Frameworks (MOFS) and Covalent Organic Frameworks (COFS) Applied to Photocatalytic Organic Transformations. *Catalysts* **2020**, *10* (7), 720.
(26) Modrow, A.; Zargarani, D.; Herges, R.; Stock, N. Introducing a Photo-Switchable Azo-Functionality inside Cr-MIL-101-NH 2 by Covalent Post-Synthetic Modification. *Dalt. Trans.* **2012**, *41* (28), 8690−8696.
(27) Alhumaimess, M. S. Metal-organic Frameworks and Their Catalytic Applications. *J. Saudi Chem. Soc.* **2020**, *24* (6), 461−473.
(28) Drisko, J. A. Chelation Therapy. *Integrative Medicine*; Elsevier, 2018; pp 1004−1015; DOI: 10.1016/B978-0-323-35868-2.00107-9.
(29) Suchecki, T. T.; Mathews, B.; Augustyniak, A. W.; Kumazawa, H. Applied Kinetics Aspects of Ferric EDTA Complex Reduction with Metal Powder. *Ind. Eng. Chem. Res.* **2014**, *53* (37), 14234−14240.
(30) Lai, T. T.; Chang, T. L. Cathodic Action of the Uranyl-EDTA Complex at the Dropping Mercury Electrode. *Anal. Chem.* **1961**, *33* (9), 1193−1196.
(31) Koehler, F. M.; Rossier, M.; Waelle, M.; Athanassiou, E. K.; Limbach, L. K.; Grass, R. N.; Günther, D.; Stark, W. J. Magnetic EDTA: Coupling Heavy Metal Chelators to Metal Nanomagnets for Rapid Removal of Cadmium, Lead and Copper from Contaminated Water. *Chem. Commun.* **2009**, No. 32, 4862.
(32) Zhao, F.; Repo, E.; Sillanpää, M.; Meng, Y.; Yin, D.; Tang, W. Z. Green Synthesis of Magnetic EDTA- And/or DTPA-Cross-Linked Chitosan Adsorbents for Highly Efficient Removal of Metals. *Ind. Eng. Chem. Res.* **2015**, *54* (4), 1271−1281.
(33) Ren, Y.; Abbood, H. A.; He, F.; Peng, H.; Huang, K. Magnetic EDTA-Modified chitosan/SiO2/Fe3O4 Adsorbent: Preparation, Characterization, and Application in Heavy Metal Adsorption. *Chem. Eng. J.* **2013**, *226*, 300−311.
(34) Sheikh Hosseini Lori, M.; Delnavaz, M.; Khoshvaght, H. Synthesizing and Characterizing the Magnetic EDTA/chitosan/CeZnO Nanocomposite for Simultaneous Treating of Chromium and Phenol in an Aqueous Solution. *Chin. J. Chem. Eng.* **2023**, *58*, 76.
(35) Jiang, Y.; Liu, C.; Huang, A. EDTA-Functionalized Covalent Organic Framework for the Removal of Heavy-Metal Ions. *ACS Appl. Mater. Interfaces* **2019**, *11* (35), 32186−32191.
(36) Gharanjik, A. A.; Alinezhad, H.; Kiani, A. EDTA-Functionalized Metal-organic Framework of TMU-16-NH2 Decorated with Pd

https://doi.org/10.1021/acsomega.4c01117
ACS Omega 2024, 9, 28114−28128

Nanoparticles as an Efficient and Effective Nanocatalyst in the Suzuki - Miyaura Coupling Reaction. *J. Mater. Sci.* **2024**, *59*, 8169.
(37) Mohammadi, M.; Ghorbani-Choghamarani, A. Complexation of Guanidino Containing L-Arginine with Nickel on Silica-Modified Hercynite MNPs: A Novel Catalyst for the Hantzsch Synthesis of Polyhydroquinolines and 2,3-Dihydroquinazolin-4(1H)-Ones. *Res. Chem. Intermed.* **2022**, *48* (6), 2641−2663.
(38) Ghorbani-Choghamarani, A.; Aghavandi, H.; Mohammadi, M. Mesoporous SBA-15@n-Pr-THAM-ZrO Organic-inorganic Hybrid: As a Highly Efficient Reusable Nanocatalyst for the Synthesis of Polyhydroquinolines and 2,3-Dihydroquinazolin-4 (1h)-Ones. *J. Porous Mater.* **2021**, *28* (4), 1167−1186.
(39) Mohammadi, M.; Ghorbani-Choghamarani, A. Synthesis and Characterization of Novel Hercynite@sulfuric Acid and Its Catalytic Applications in the Synthesis of Polyhydroquinolines and 2,3-Dihydroquinazolin-4(1: H)-Ones. *RSC Adv.* **2022**, *12* (5), 2770−2787.
(40) Kazemi, M.; Mohammadi, M. Magnetically Recoverable Catalysts: Catalysis in Synthesis of Polyhydroquinolines. *Appl. Organomet. Chem.* **2020**, *34* (3), No. e5400.
(41) Shadmehr, J.; Zeinali, S.; Tohidi, M. Synthesis of a Chromium Terephthalate Metal Organic Framework and Use as Nanoporous Adsorbent for Removal of Diazinon Organophosphorus Insecticide from Aqueous Media. *J. Dispers. Sci. Technol.* **2019**, *40* (10), 1423−1440.
(42) García-Ramos, J. C.; Galindo-Murillo, R.; Tovar-Tovar, A.; Alonso-Saenz, A. L.; Gómez-Vidales, V.; Flores-Álamo, M.; Ortiz-Frade, L.; Cortes-Guzmán, F.; Moreno-Esparza, R.; Campero, A.; Ruiz-Azuara, L. The π-Back-Bonding Modulation and Its Impact in the Electronic Properties of Cu II Antineoplastic Compounds: An Experimental and Theoretical Study. *Chem. - A Eur. J.* **2014**, *20* (42), 13730−13741.
(43) Oguadinma, P. O.; Schaper, F. π Back-Bonding in Dibenzyl-β-Diketiminato Copper Olefin Complexes. *Organometallics* **2009**, *28* (23), 6721−6731.
(44) Khramov, D. M.; Lynch, V. M.; Bielawski, C. W. N-Heterocyclic Carbene-Transition Metal Complexes: Spectroscopic and Crystallographic Analyses of π-Back-Bonding Interactions. *Organometallics* **2007**, *26* (24), 6042−6049.
(45) Miao, X.-H.; Xiao, H.-P.; Zhu, L.-G. Poly[zinc(II)-μ 2 −4,4′-Bipyridine-Di-μ 2 -Formato]: A Chiral Three-Dimensional Coordination Polymer. *Acta Crystallogr. Sect. E Struct. Reports Online* **2006**, *62* (8), m1756−m1757.
(46) Abdollahi-Basir, M. H.; Mirhosseini-Eshkevari, B.; Zamani, F.; Ghasemzadeh, M. A. Synthesis of tetrazolo[1,5-A]pyrimidine-6-Carbonitriles Using HMTA-BAIL@MIL-101(Cr) as a Superior Heterogeneous Catalyst. *Sci. Rep.* **2021**, *11* (1), 5109.
(47) Zhong, R.; Yu, X.; Meng, W.; Liu, J.; Zhi, C.; Zou, R. Amine-Grafted MIL-101(Cr) via Double-Solvent Incorporation for Synergistic Enhancement of CO 2 Uptake and Selectivity. *ACS Sustain. Chem. Eng.* **2018**, *6* (12), 16493−16502.
(48) Babaee, S.; Zarei, M.; Sepehrmansourie, H.; Zolfigol, M. A.; Rostamnia, S. Synthesis of Metal-Organic Frameworks MIL-101(Cr)-NH 2 Containing Phosphorous acid Functional Groups: Application for the Synthesis of N -Amino-2-Pyridone and Pyrano [2,3-c]Pyrazole Derivatives via a Cooperative Vinylogous Anomeric-Based Oxidation. *ACS Omega* **2020**, *5* (12), 6240−6249.
(49) Ghorbani-Choghamarani, A.; Aghavandi, H.; Mohammadi, M. Mesoporous SBA-15@n-Pr-THAM-ZrO Organic-inorganic Hybrid: As a Highly Efficient Reusable Nanocatalyst for the Synthesis of Polyhydroquinolines and 2,3-Dihydroquinazolin-4 (1h)-Ones. *J. Porous Mater.* **2021**, *28* (4), 1167−1186.
(50) Pasinszki, T.; Krebsz, M.; Lajgut, G. G.; Kocsis, T.; Kótai, L.; Kauthale, S.; Tekale, S.; Pawar, R. Copper Nanoparticles Grafted on Carbon Microspheres as Novel Heterogeneous Catalysts and Their Application for the Reduction of Nitrophenol and One-Pot Multicomponent Synthesis of Hexahydroquinolines. *New J. Chem.* **2018**, *42* (2), 1092−1098.
(51) Ghorbani-Choghamarani, A.; Heidarnezhad, Z.; Tahmasbi, B.; Azadi, G. TEDETA@BNPs as a Basic and Metal Free Nanocatalyst for Knoevenagel Condensation and Hantzsch Reaction. *J. Iran. Chem. Soc.* **2018**, *15* (10), 2281−2293.
(52) Bielejewski, M.; Ghorbani, M.; Zolfigol, M. A.; Tritt-Goc, J.; Noura, S.; Narimani, M.; Oftadeh, M. Thermally Reversible Solidification of Novel Ionic Liquid [im]HSO4 by Self-Nucleated Rapid Crystallization: Investigations of Ionic Conductivity, Thermal Properties, and Catalytic Activity. *RSC Adv.* **2016**, *6* (110), 108896−108907.
(53) Abedini, M.; Shirini, F.; Mousapour, M. Poly-(vinylpyrrolidinium) Perchlorate as a New and Efficient Catalyst for the Promotion of the Synthesis of Polyhydroquinoline Derivatives via Hantzsch Condensation. *Res. Chem. Intermed.* **2016**, *42* (3), 2303−2315.
(54) Singh, H.; Garg, N.; Arora, P.; Rajput, J. K.; Jigyasa. Sucrose Chelated Auto Combustion Synthesis of BiFeO 3 Nanoparticles: Magnetically Recoverable Catalyst for the One-pot Synthesis of Polyhydroquinoline. *Appl. Organomet. Chem.* **2018**, *32* (6), No. e4357.
(55) Vaysipour, S.; Rafiee, Z.; Nasr-Esfahani, M. Synthesis and Characterization of Copper (II)-Poly(acrylic acid)/M-MCM-41 Nanocomposite as a Novel Mesoporous Solid Acid Catalyst for the One-Pot Synthesis of Polyhydroquinoline Derivatives. *Polyhedron* **2020**, *176*, 114294.
(56) Mayurachayakul, P.; Pluempanupat, W.; Srisuwannaket, C.; Chantarasriwong, O. Four-Component Synthesis of Polyhydroquinolines under Catalyst- and Solvent-Free Conventional Heating Conditions: Mechanistic Studies. *RSC Adv.* **2017**, *7* (89), 56764−56770.
(57) Moosavi-Zare, A. R.; Zolfigol, M. A.; Zarei, M.; Zare, A.; Afsar, J. Design, Characterization and Application of Silica-Bonded Imidazolium-Sulfonic Acid Chloride as a Novel, Active and Efficient Nanostructured Catalyst in the Synthesis of Hexahydroquinolines. *Appl. Catal. A Gen.* **2015**, *505*, 224−234.
(58) Rakhtshah, J.; Salehzadeh, S.; Zolfigol, M. A.; Baghery, S. Synthesis, Characterization and Heterogeneous Catalytic Application of a nickel(II) Schiff Base Complex Immobilized on MWCNTs for the Hantzsch Four-Component Condensation. *J. Coord. Chem.* **2017**, *70* (2), 340−360.
(59) Khazaei, A.; Mahmoudiani Gilan, M.; Sarmasti, N. Magnetic-based Picolinaldehyde-melamine Copper Complex for the One-pot Synthesis of Hexahydroquinolines via Hantzsch Four-component Reactions. *Appl. Organomet. Chem.* **2018**, *32* (3), No. e4151.
(60) Khazaei, A.; Sarmasti, N.; Seyf, J. Y.; Tavasoli, M. Synthesis of Hexahydroquinoline (HHQ) Derivatives Using ZrOCl 2 ·8H 2 O as a Potential Green Catalyst and Optimization of Reaction Conditions Using Design of Experiment (DOE). *RSC Adv.* **2015**, *5* (123), 101268−101275.
(61) Dharma Rao, G. B.; Nagakalyan, S.; Prasad, G. K. Solvent-Free Synthesis of Polyhydroquinoline Derivatives Employing Mesoporous Vanadium Ion Doped Titania Nanoparticles as a Robust Heterogeneous Catalyst via the Hantzsch Reaction. *RSC Adv.* **2017**, *7* (6), 3611−3616.
(62) Ramish, S. M.; Ghorbani-Choghamarani, A.; Mohammadi, M. Microporous Hierarchically Zn-MOF as an Efficient Catalyst for the Hantzsch Synthesis of Polyhydroquinolines. *Sci. Rep.* **2022**, *12* (1), 1479.
(63) Ghorbani-Choghamarani, A.; Mohammadi, M.; Shiri, L.; Taherinia, Z. Synthesis and Characterization of Spinel FeAl2O4 (Hercynite) Magnetic Nanoparticles and Their Application in Multicomponent Reactions. *Res. Chem. Intermed.* **2019**, *45* (11), 5705−5723.
(64) Tamoradi, T.; Ghadermazi, M.; Ghorbani-Choghamarani, A. Ni(II)-Adenine Complex Coated Fe3O4 Nanoparticles as High Reusable Nanocatalyst for the Synthesis of Polyhydroquinoline Derivatives and Oxidation Reactions. *Appl. Organomet. Chem.* **2018**, *32* (1), No. e3974.

https://doi.org/10.1021/acsomega.4c01117
ACS Omega 2024, 9, 28114−28128

(65) Saadati-Moshtaghin, H. R.; Zonoz, F. M. Preparation and Characterization of Magnetite-Dihydrogen Phosphate as a Novel Catalyst in the Synthesis of Tetrahydrobenzo[b]pyrans. *Mater. Chem. Phys.* **2017**, *199*, 159−165.
(66) Taheri, N.; Heidarizadeh, F.; Kiasat, A. A New Magnetically Recoverable Catalyst Promoting the Synthesis of 1,4-Dihydropyridine and Polyhydroquinoline Derivatives via the Hantzsch Condensation under Solvent-Free Conditions. *J. Magn. Magn. Mater.* **2017**, *428*, 481−487.
(67) Pourian, E.; Javanshir, S.; Dolatkhah, Z.; Molaei, S.; Maleki, A. Ultrasonic-Assisted Preparation, Characterization, and Use of Novel Biocompatible Core/Shell Fe3O4@GA@Isinglass in the Synthesis of 1,4-Dihydropyridine and 4 H-Pyran Derivatives. *ACS Omega* **2018**, *3* (5), 5012−5020.

https://doi.org/10.1021/acsomega.4c01117
ACS Omega 2024, 9, 28114−28128